Characteristics of Two Types of Grazing Incidence Spectrometers with Holographic Gratings

By

Hidetoshi SUEMITSU*, Toshifumi HASAMA* and Kuniya FUKUDA*

(Received March 29, 1980)

Abstract

Two types of grazing incidence spectrometers have been constructed which are applicable to photographic and photo-electric recordings of emission spectra of plasmas in the extreme ultraviolet. The spectrometer SGX-100 with a 1-m Rowland circle covers the wavelengths of 30 to 1500 Å with both a holographic grating (HG) and a ruled one (RG). In this spectrometer, the incidence angle α to the gratings is continuously variable from 80° to 86°, where the inverse Vodar mounting is adopted to keep a constant line of sight of the spectrometer against a light source. The small grazing incidence spectrometer GIT-30 with a toroidal holographic grating covers the wavelengths of 150 to 1600 Å. The wavelength scanning is performed by a simple rotation of the grating under a constant angle 142° between the incident and exit beams. These spectrometers were used to observe spectra of emissions from a hollow cathode lamp and linear Z-pinch and plasma-focus discharges. Characteristics of the spectrometers are discussed on the data observed.

§1. Introduction

Plasma spectroscopy in the extreme ultraviolet (XUV) is very important in diagnosis as well as in studies of atomic processes of high temperature plasmas. Particularly in thermonuclear fusion (TF) plasmas, many kinds of high-Z impurity ions such as C-, N-, O- and metal-ions emit intense radiation in the XUV,[1-4] which leads to a serious problem of radiation loss in the attainment of TF reaction. In this connection much attention has been directed to the spectroscopic studies of excitation and ionization of high-Z ions in plasmas in the XUV,[5,6] and also to the XUV spectroscopy of high-Z ions, such as beam-foil spectroscopy,[7] and solar spectroscopy.[8]

Early work of XUV spectroscopy on TF plasmas was carried out at the Culham Laboratory with a 1-m grazing incidence vacuum spectrometer E580 (Hilger Watts Ltd.).[9] This vertical-type spectrometer with a horizontal entrance slit

* Department of Engineering Science

had a photographic plate holder and a photo-electric detector, but it was mainly used as a spectrograph. In this spectrometer, a ruled grating (RG) of groove density $N_G=600$ lines/mm and a blaze angle $\alpha_B=1°\ 30'$ was employed, and a wavelength of 5 to 950 Å was covered. The angle of incidence α to the grating was variable at discrete values of 86°, 88° and 89°. In the Princeton Plasma Physics Laboratory (PPPL), temporal behaviors of high-Z impurity ions in ST and PLT tokamak plasmas have been observed with a 1-m grazing incidence spectrometer GISMO (SPEX Inc.).[1,10] The spectrometer is employed as a spectrograph with a daylight loading 35 mm camera covering the wavelength region from 0 to 2400 Å, and as a monochromator with two photo-electric detector-heads independently driven along the Rowland circle. A RG and a holographic grating (HG), both $N_G=1200$ lines/mm, are interchangeable, and the angle α is continuously variable from 80° to 86°.

The TFR group (French tokamak at Fontenay-aux-Rose) has estimated the radiation loss due to high-Z impurity ions in the tokamak with a grazing incidence duochromator in the wavelength ragion of 100 to 1300 Å.[2] Very recently, in collaboration with the Raca Institute group, they have assigned an Mo pseudo-continuum with a 2-m grazing incidence spectrograph in the wavelength region of 5 to 100 Å ($\alpha=89°$ and $N_G=2400$ lines/mm).[3,4] In the XUV spectroscopy on laboratory plasmas, various spectrographs and monochromators with low or high resolutions have been used in a limited or a wide wavelength region, depending on research subjects such as the determination of effective ionization rates of high-Z ions,[5,6] the measurement of polarization shifts of excited levels of hydrogenic ions,[11,12] the observation of XUV spectra of high-Z ions produced by laser irradiation[13] etc. As for commercial instruments, a 1-m McPherson monochromator has been widely used, while recently a high-resolution spectrograph GML 5M (Grating Measurements Ltd.)[14] and a small-size monochromator (Jobin-Ivon Inc.)[15,16] have been developed.

This paper describes two types of grazing incidence spectrometers which have been newly constructed to observe XUV radiation from various kinds of plasmas, and also to measure collision induced XUV emissions in ion-beam experiments in our laboratory. One is a grazing incidence spectrometer SGX-100 with a 1-m Rowland circle, which covers the wavelength region from 30 to 1500 Å with both an HG and an RG. The other is a small grazing incidence spectrometer GIT-30 with a toroidal HG which covers a wavelength region from 150 to 1600 Å. These spectrometers are both applicable to photographic and photo-electric recordings of plasma emissions. The latter is also available as a monochromator. In the next section, details of the spectrometers are described together with the light sources of linear Z-pinch and plasma-focus discharges. In §3, observed spectra are presented so that the characteristics of the spectrometers can be discussed in detail.

§2. Experiment

2-1 The spectrometer SGX-100 with the 1-m Rowland circle

The grazing incidence 1-m vacuum spectrometer SGX-100 works as a spectrograph with a photographic camera and as a monochromator with a photoelectric detector-head. A daylight loading Kodak-SWR film holder is vertically shifted in the camera to permit eight exposures of spectra 210 mm wide and 3 mm high. The camera is driven along a 1-m Rowland circle to cover the wavelegth region of 50 to 1500 Å. The photo-electric detector-head with an exit slit of a fixed width 50 μ, which is easily interchangeable with the camera, scans the wavelength region of 30 to 1500 Å. A wide choice of detectors is possible, but in the present experiment an electron multiplier HTR 595 with Cu-Be photocathode was used. A bilateral entrance slit opens from 0 to 1 mm by operation from outside the vacuum tank.

An RG (the blaze angle $\alpha_B=1°$, and the blaze wavelength $\lambda_B=290$ Å) and an HG, both Pt-coated and of $N_G=1200$ lines/mm, are easily interchangeable. The incidence angle α to the gratings is continuously variable from 80° to 86° without changing the incidence-beam direction to the gratings from a plasma light source through the entrance slit. This is made possible by making use of the inverse Vodar mounting as shown in Figs. 1 and 2. In Fig. 1, the lines XX′ and YY′ show the direction of the guide rails (9 in Fig. 2) along which moves an arc GA of a constant length of the Rowland circle.

In the following the numbers in parentheses refer to the numbers in Fig. 2. An entrance slit (6) is at point S_1, the intersection point of XX′ and YY′, and the center of the grating (5) is at point G. Then, for example, when the arc GA

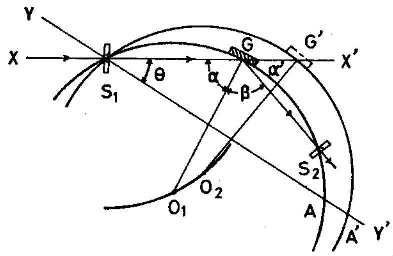

Fig. 1. Schematic representation of the mounting of SGX-100 spectrometer.

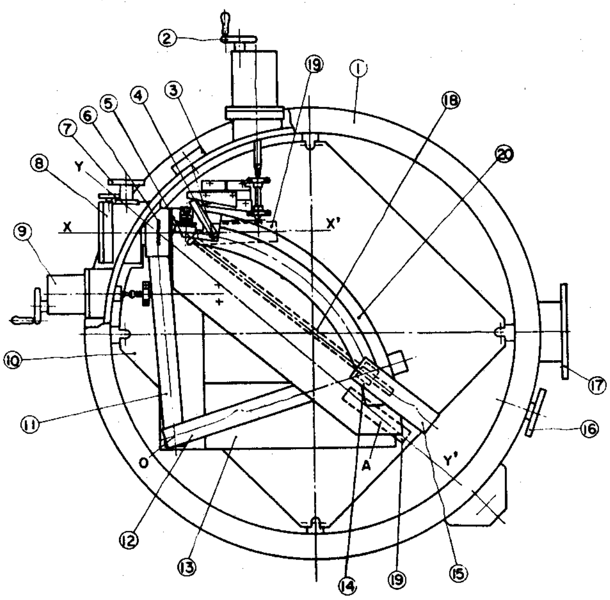

Fig. 2. Set-up of the Mounting of SGX-100 spectrometer.

moves to the position G'A', the center of the Rowland circle O_1 moves to O_2, the grating center G shifts to G', and the angle α changes to α'. However, the optical axis XS_1G (or XS_1G') of the incidence-beam to the spectrometer remains unchanged. For any angle α, a small mirror (4) near the grating reflects the zeroth-order light out of a window (3) of the vacuum tank (1). The variation of α under a constant incidence-beam axis, which is accomplished by the movement of a plate (13) along the guide (19) with a handle (9), makes it possible to filter out overlapping orders of a spectrum, or to examine the α-dependence of the efficiency (or through-put) of a grating.

For a given α, the arm OS_2 (12) defines a point S_2, the position of the exit slit S_2 (14) or the center of the film plane, on the Rowland circle. A fine screw (18) along the line GS_2 drives the photo-electric detector-head (15) or the camera along the Rowland circle on a plate (20), where the handle (2) is set for manual driving. The speed of the wavelength scanning is varied in 10 steps by a pulse motor, or controlled by a synchronous motor depending on the experimental conditions. For example, when a repetitive discharge operates the linear Z-pinch plasma light source, the discharge pulse disturbed the pulse-motor driving. The vertical shift of the film holder and shutter movement of the camera are electrically operated from outside the vacuum tank.

The vacuum tank is evacuated down to 1×10^{-6} Torr through a pneumatic valve with a 400 l/sec diffusion pump connected to a 640 l/min mechanical booster pump and a 300 l/min rotary pump in series. Differential pumping is feasible between a gate valve (8) and the entrance slit (6). The terminals of high-voltage supplies and signal outputs for the HTR-595 electron multiplier are at the center of the bottom of the vacuum tank. The tank with the diffusion pump is vertically positioned by an oil-hydraulic lift.

2-2 The small spectrometer GIT-30 with a toroidal HG

Figure 3 depicts the schematic diagram of the mounting of the small grazing incidence spectrometer GIT-30 when used as a monochromator, where a camera attachment is also shown. The spectrometer is equipped with an Au-coated Jobin-Yvon toroidal HG (1 in Fig. 3) of $N_G=550$ lines/mm and the ruled area 30×30 mm. The grating has a greater radius of curvature 1 m in the horizontal position, and a lesser radius 107 mm in the vertical position. In the following, the numbers in parentheses refer to the numbers in Fig. 3. A diaphragm (2) is set in front of the grating to limit the shape and size of the aperture for the HG. Plates having a slit of adjustable width are inserted into the slit-boxes (3). The entrance slit-box is connected to a light source (4) (a hollow cathode lamp in Fig. 3), and the exit slit-box to a vacuum chamber (5) including an HTR 595 electron-multiplier. Differential pumping is feasible in front of the entrance slit-box and behind the exit slit-box.

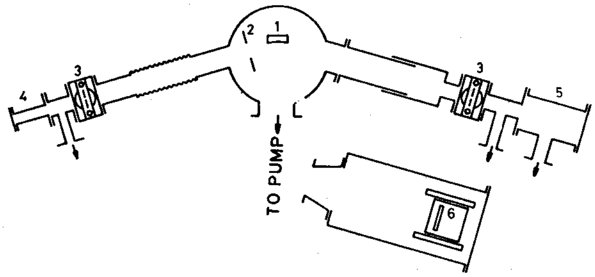

Fig. 3. The mounting of GIT-30 spectrometer.

The entrance slit is fixed at 320 mm from the center of the HG, whereas the exit slit is movable along the exit-beam axis between 300 and 330 mm from the center of the HG. The angle between the entrance- and exit-beam axes is fixed at 142°, while a simple rotation of the HG around the vertical axis through the grating center gives the wavelength scanning. A pulse motor or a synchronous motor drives the scanning. When the spectrometer is employed as a spectrograph, a camera attachment including a film-holder is set in place of the exit-beam arm.

The film-holder is allowed to translate along and to tilt against the exit-beam axis. The spectrometer is evacuated down to 1×10^{-5} Torr or lower when operated with a hollow-cathode or plasma light sources.

2-3 Observation of spectra with the spectrometer SGX-100

First, the SGX-100 was operated with a hollow-cathode light source to obtain photographic and photo-electric recordings of the spectra of HeI and II and some impurities of O and N. The adjustment and calibration of the spectrometer with the RG and HG were performed at various angles α in the region from 1500 Å to HeII Ly-6 234 Å. The focusing was adjusted in the spectrograph mode, and the wavelengths were calibrated on counter numbers for driving the camera or the photo-electric detector-head. The effect of the cut-off mirror was examined for zeroth-order light scattering, etc. Next, a linear Z-pinch plasma light source was employed for the adjustment and calibration of the spectrometer in the wavelength region down to about 50 Å.

A linear pinch discharge in rare gases with a moderate imput energy, e.g. $C=2$–$3\ \mu F$ and $V=15$–20 kV, is available as a XUV light source on a laboratory scale.[17,18] In the present experiment, discharges in He gases mixed with a small amount (the order of 0.1 mol%) of N_2, O_2, CO_2, and SF_6 were used, which gave many spectral lines of C-, N-, O-, F- and S-ions in various ionization stages.[19,20] The linear Z-pinch discharge tube and experimental set-up were the same as described in the previous paper on an experiment with a Seya-Namioka mounting spectrometer.[17] Mixed gas was made to flow through the discharge tube from a mixing tank by differential pumping in front of the entrance slit, and the pressure in the tube was varied from 0.1 to 1 Torr. The spectrometer was evacuated to a pressure of 1×10^{-5} Torr or lower.

The assignment to spectroscopic terms and classification to isoelectronic sequences were carried out on many lines of photographed spectra of plasmas produced from He-N_2, -O_2,-CO_2 and -SF_6 gases. The appearance of the spectra differed depending on the grating employed, an RG or an HG, which is considered to reflect the efficiency of the grating. For comparison, spectra of He-O_2 plasma were photographed over a wide wavelength region with the RG and with the HG at various values of angle α under the same discharge conditions of the linear Z-pinch tube. Furthermore, five spectral lines, HeII 304 Å, OIV 780, 554 and 116 Å, and OV 204 Å were selected, and the intensity variation of these lines was plotted as a function of α for the RG and HG, where the characteristic curve of Kodak SWR films was made at the five wavelengths, assuming that the exposure was proportional to the shot numbers of the pinch discharges.

The photo-electric observation with the spectrometer SGX-100 was performed on He-O_2 plasma with an electron-multiplier HTR 595. Temporal behaviors of several spectral lines of HeII and OII to VI ions and continuum emission from the He-O_2 pinch plasma were measured at various pressures from 0.1 to 1 Torr. The pressure giving the maximum pinch[21] was 0.4 Torr for the present condition of the discharges.

2-4 Observation of spectra with the spectrometer GIT-30

A toroidal grating is designed to eliminate astigmatism which becomes conspicuous in the case of grazing incidence. Experimental as well as computational examinations are necessary to find a critical condition for the mounting of the grating which gives a compromise between the elimination of astigmatism and the growth of other aberrations such as coma. Since the Jobin-Yvon group does not give any information about this point, we performed an experiment to find the critical condition.

First, a spectrometer GIT-30 with the toroidal HG was used as a spectrograph with a camera attachment. The width of the entrance slit was set at 40 μm, and using the hollow-cathode light source, images of the entrance slit were photographed at various wavelengths, e.g. 0 Å (zeroth-order light), HeII 304 Å, HeI 584 Å and some O-lines, in the negative order by varying the distance of the film-plane from the grating center, the tilting angle of the film-plane against the exit-beam axis, and the shape and size of the diaphragm in front of the HG, where the angle between the incident- and exit-beams was, of course, kept at 142°. A single critical condition acceptable in the wavelength region from 300 to 1400 Å was determind by examining many spectrograms. Then, the spectrometer was used as a monochromator, and the critical condition was again checked by recording the photo-electric spectra of emission from the hollow-cathod light source under various conditions of the monochromator. Finally, the spectrometer was also used as a spectrograph under the critical condition to observe the spectra of emission from a plasma-focus light source.

The plasma-focus light source of a Maser type[22,23] had an inner-electrode (Cu,Al,Fe) of 17 mm in diameter and 140 mm in length, and a concentric outer-tube-electrode (Cu) of 40 mm in diameter and 140 mm in length. Helium or H_2 gas was introduced into the light source and made to flow at a pressure of 0.2 to 5 Torr by differential pumping in front of the entrance slit-box. A capacitor bank of $C=10$ μF and $L=100$ nH fed the current to the light source with $V=15$ to 20 kV. The current was underdamped with an initial peak 170 kA. Light emission from the focused plasma was observed through a hole (2 mm diameter) of a Boron-Nitride (BN) cylinder fitting the window of the light source. This small hole prevented plasma flow from coming into the spectrograph. Details of the plasma-focus light source will be described elsewhere.

§3. Results and discussions

3-1 Characteristics of the spectrometer SGX-100

Figure 4 shows the zeroth-order light scattering from the RG, detected at three angles of incidence with a solar-blind HTR-595 electron multiplier using a hollow-cathode light source. It is seen that a complete cut-off and a half-shadow of the cut-off mirror shift towards a shorter wavelength with some changes in the scattered light intensity in the spectrum as the angle α is increased.

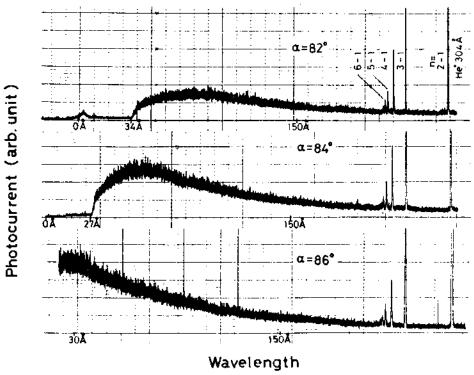

Fig. 4. Zeroth-order light scattering at three values of the incident angle α to the RG.

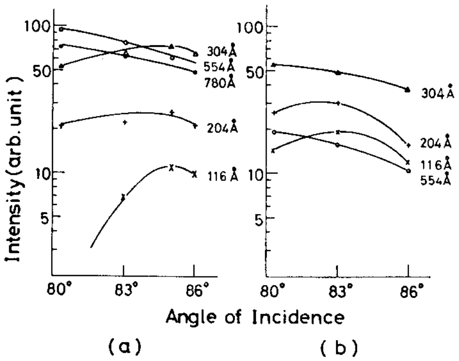

Fig. 5. Intensities of the five lines, HeII 304Å, OIV 780, 554 and 116 A, and OV 204 Å, as a function of the angle α (a) for the HG and (b) for the RG.

Figure 5 (a and b) shows the intensities of the five spectral lines, HeII 304 Å, OIV 780, 554 and 116 Å, and OV 204 Å, as a function of the angle α for the HG and RG, respectively. Here, the relative intensity of each line with respect to α is determined by means of densitometry of the photographed spectra, but the relative intensity among the five lines is not calibrated. Figure 6 shows the microdensitometer traces of the wide-range spectra of the impurity O-ions in He plasma, photographed with the RG and HG under the same discharge condition: 40 shots exposure of pinch discharges with $C=3\ \mu F$ and $V=20$ kV in He-O_2 (0.5 mol%) gas at a pressure $p=0.2$ Torr. In the spectrum taken with the HG, the correspondence among the spectral lines of the first, second and third orders is indicated by the numbers on the upper scale, whereas no marked higher-order lines exist in the spectrum taken with the RG.

Figures 5 and 6 indicate that the HG has a high efficiency over a much wider

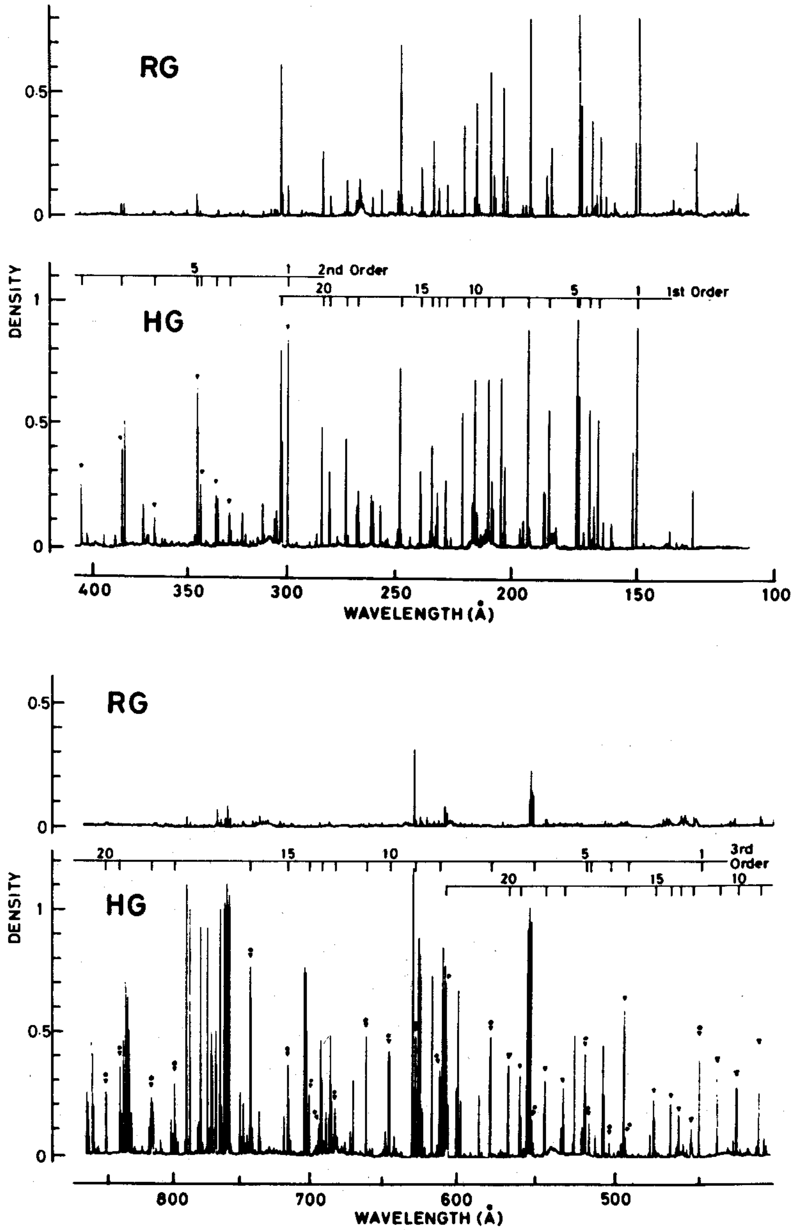

Fg. 6. Micro-denisitometer traces of wide-range spectrograms of impurity O-ion lines in linear pinch He-plasma (He-O_2: $V=20$ kV, $C=3\ \mu F$ and $p=0.2$ Torr), photographed with the RG and HG.

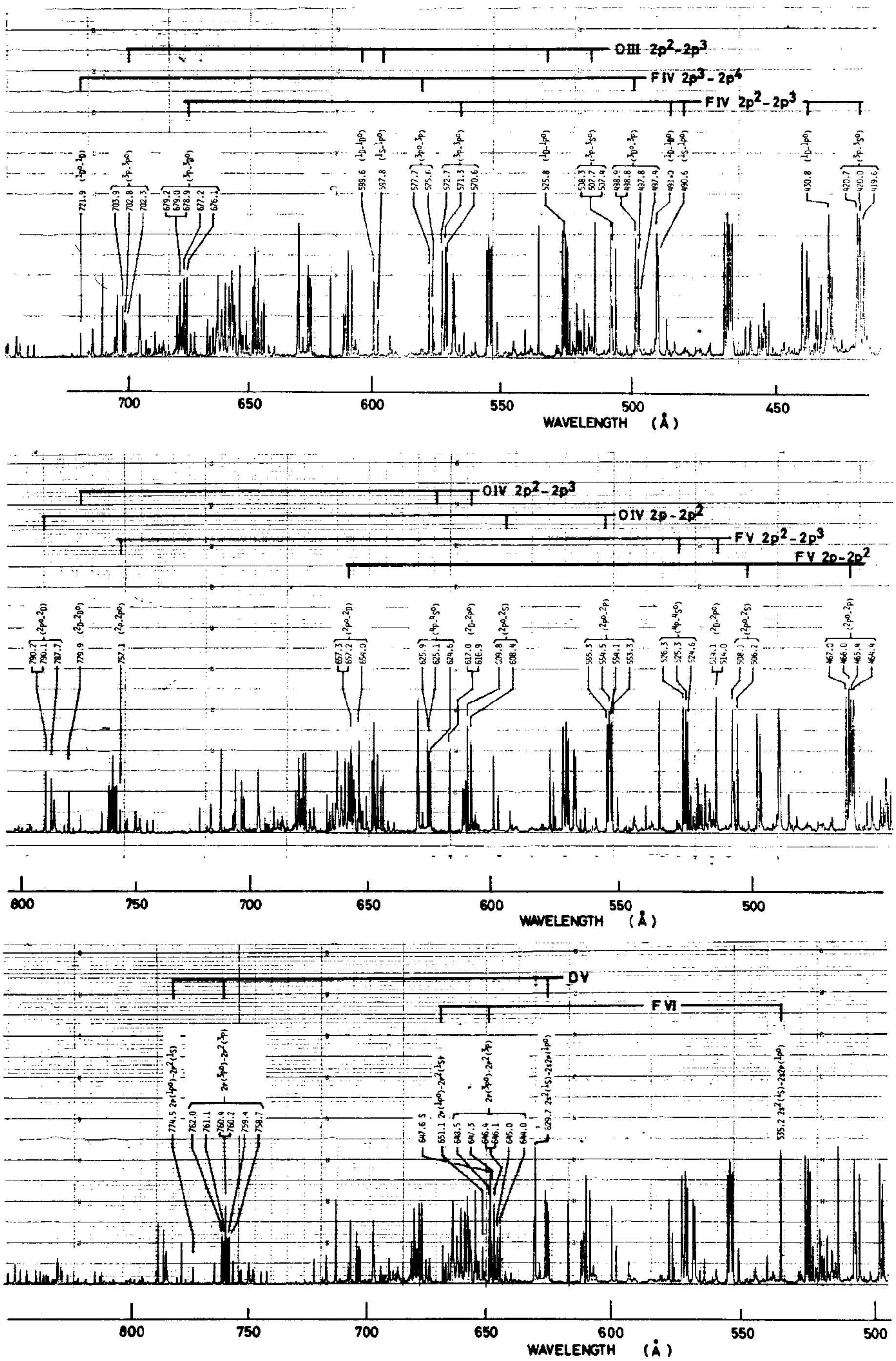

Fig. 7. Assignment of emission lines of iso-electronic ions, FIV to VI-ions and OIII to V-ions, in linear pinch He-plama (He-SF_6: V=20 kV, C=3 μF and p=0.2 Torr) on microdensitometer traces of spectrogram taken with the HG in 400 to 800 Å.

wavelength range (100 to about 1500 Å) than the RG (100 to about 500 Å). The HG gives rise to strong lines of the second and third order. The RG (blaze angle= 1° and blaze wavelength=290 Å) does not show a strong dependence of efficiency on the angle α. The efficiency at the short wavelength limit (200 to 100 Å) becomes maximum at $\alpha=83°$ as shown in Fig. 5 (b). The HG (with no specification by Jobin-Yvon) has a wide wavelength-range efficiency similar to grating No. 9 of ref. 24 with a groove depth of 520 Å. However, it gives rise to the third-order spectrum comparable to, or more intense than the second-order spectrum for the lines with the numbers 7 to 17 in $\lambda=190$ to 270 Å, as shown in Fig. 5. The efficiency of the HG at its short wavelength limit strongly depends on the angle α as seen by the 116 Å line in Fig. 5 (a).

Figure 7 shows the assignment of the FIV- to VI-ion lines and the OIII- to V-ion lines on the micro-densitometer traces of the spectrum ($\lambda=400$ to 800 Å), photographed by 40 shots discharged in He-SF_6 (0.1 mol%) with the HG at $\alpha=$ 83°. The spectrum also includes weak OII-ion lines[19] and higher-order lines. Figure 8 shows the assignment of the FVI- and VII-ion lines and the SVII-ion lines on the micro-densitometer traces of the spectrum ($\lambda=50$ to 300 Å), photographed by 50 shots discharged in He-SF_6 (0.1 mol%) with the RG at $\alpha=83°$. The spectrum also includes FIV- and V-ion lines and O-ion lines. In the both cases, the discharges were made at p=0.2 Torr with C=3 μF and V=20 kV.

As shown in the three separate traces of the same spectrum in Fig. 7, the corresponding iso-electronic transitions are clearly seen in the ions with an iso-electronic configuration: OIII and FIV ($2s^22p^2$: $^3P_0$), OIV and FV ($2s^22p$: $^2P^o_{1/2}$), and OV and FVI ($2s^2$: $^1S_0$), where the electronic configurations and spectroscopic term-symbols of the ground states are shown in parentheses. In these traces, the configurations $2s^22p^m$ and $2s2p^{m+1}$ are written without any designations of the 2s-electron except for 2s2p and $2s^2$ for m=0 to 2. The reciprocal linear dispersion of the spectrometer is calculated as 1.6, 3.0 and 3.7 Å/mm at 100, 500 and 800 Å, respectively. In the spectrum of Fig. 7, (the entrance-slit width = 30 μm), a line-separation of about 0.2 Å or smaller is not resolved. For example, 5 lines are observed for the 6 fine-structure lines at $\lambda=758.7$ to 762.0 Å of OV and $\lambda=644.0$ to 648.5 Å of FVI for the transitions $2p^2\,^3P-2s2p^3P^o$. In the spectrum around 100 Å in Fig. 8, a line-separation of 0.1 Å or smaller is not discriminated as seen for several transitions of FVI-and VII-ions.

Examples of photo-electric recordings of emission spectra are shown in ref.25 for O-ion lines in linear-pinch He plasma produced from He-O_2 gas. Details of ionization of O-ions in the He plasma will be described in a forthcoming paper, in relation to the photoelectric recording of the O-ion lines.

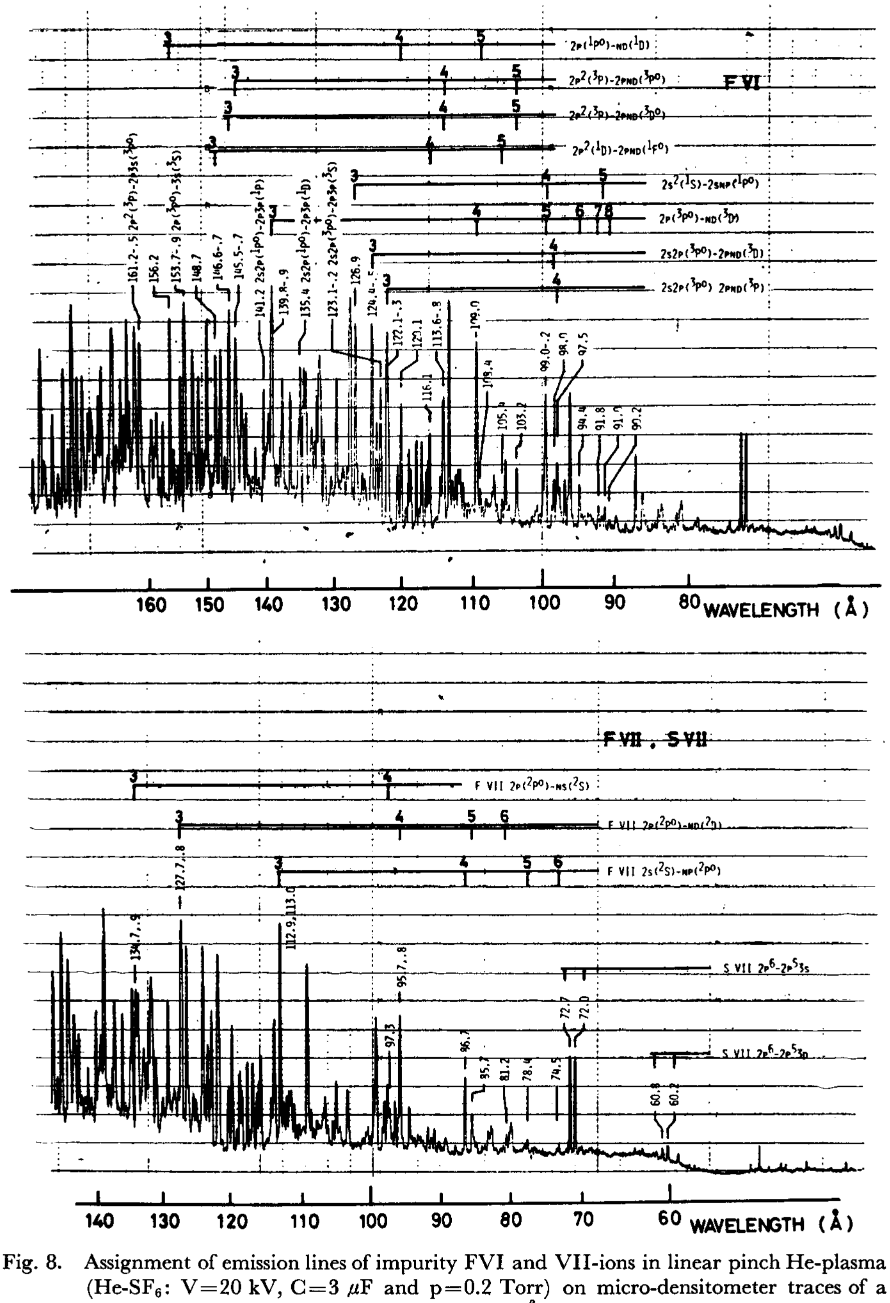

Fig. 8. Assignment of emission lines of impurity FVI and VII-ions in linear pinch He-plasma (He-SF_6: V=20 kV, C=3 μF and p=0.2 Torr) on micro-densitometer traces of a spectrogram taken with the HG in λ50 to 180 Å.

3-2 Characteristics of the spectrometer GIT-30

Figure 9 shows images of the entrance slit for HeII Lyman-lines from the hollow-cathode light source at the distance d=305 and 330 mm of the film-plane from the HG center. The width and the height of the slit are w=40 μm and h=8 mm, respectively. The aperture of the diaphargm does not limit the ruled area of the HG, i.e., the effective area of the HG is A=30×30 mm. The toroidal HG employed had the mark of an arrow on the backside. When the arrow pointed toward the direction of the incident (or diffracted) beam, we considered the HG to be in a correct position for mounting. In fact, when the HG was turned upside-down from the reverse to the correct position at a fixed d-value, the image of the entrance slit became much improved as shown in Fig. 9. Furthermore, when the tilt-angle, the angle between the normal of the film-plane and the exit-beam

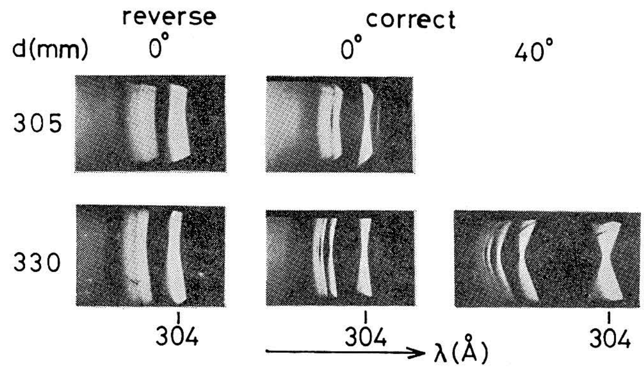

Fig. 9. Changes in the image of the entrance slit (width w=40 μm, height h=8 mm) for HeII Lyman-lines against the distance d and the tilt-angle θ of the film-holder and the direction of the HG in the negative order.

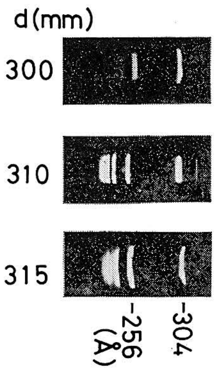

Fig. 10. Center-images of the entrace slit (w=40 μm, h=1.2 mm) for HeII Lyman-lines at d=300, 310 and 315 mm for θ=0°.

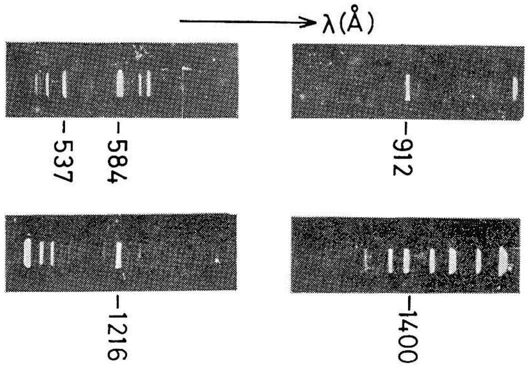

Fig. 11. Center-images of the entrance slit (w=40 μm, h=1.2 mm) for λ=580, 910, 1200 and 1400 Å at d=310 mm with θ=0°.

axis, was changed from $\theta=0°$ 40°, the coma aberration became quite marked as shown in the figure.

Figure 10 shows the center-part of the images of the entrance slit (w=40 μm, h=1.2 mm) for HeII Lyman-lines at d=300, 310 and 315 mm for $\theta=0°$, where the aperture of the diaphragm limits the effective area of the HG to A=10×10 mm. For the HeII 304 Å resonance-line, at d=310 mm the shape of the slit image is nearly symmetric and its height is approximately equal to that of the entrance slit. That is to say, that the image is stigmatic, in contrast to the curved and somewhat enlarged images at d=300 and 315 mm. In general, the image produced by the HG was improved when the diaphragm aperture limited the height of the HG effective area to a smaller value. We fixed the distance at d=310 mm, and rotated the HG to take spectrograms at various wavelengths for $\theta=0°$ with A=10×10 mm. Figure 11 shows the images of the entrance slit (w=40 μm, h=1.2 mm) in the wavelength ranges centered at about 580, 910, 1200 and 1400 Å. These images at the center wavelengths are approximately stigmatic and have a symmetric form.

We tried to take spectrograms of emission from the plasma-focus light source with a spectrometer GIT-30 for d=310 mm, w=40 μm, h=1.2 mm and $\theta=0°$. Figure 12 is an example of the spectrogram of emission from the plasma-focus discharges in helium with the Al-anode at the pressure p=4 Torr with C=10 μF

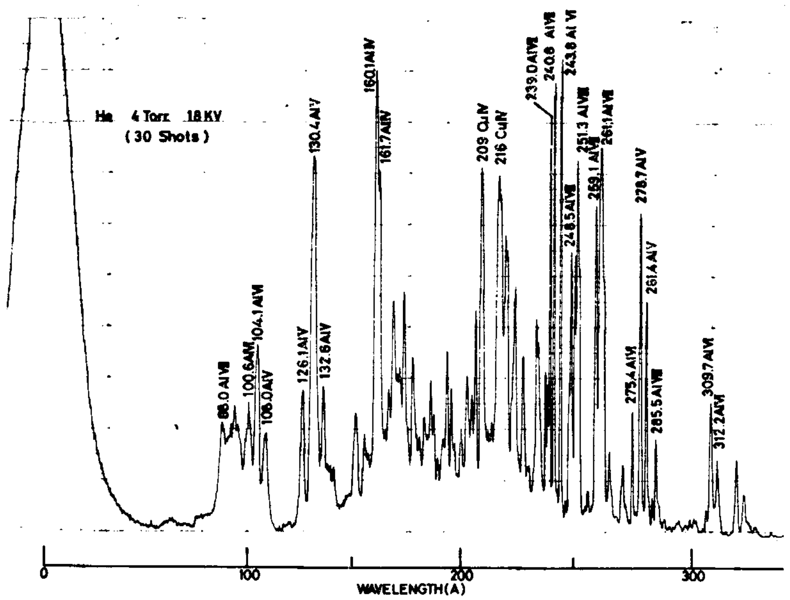

Fig. 12. Spectrum of emission from the plasma-focus discharge with Al-anode in He at p=4 Torr (C=10 μF, V=18 kV).

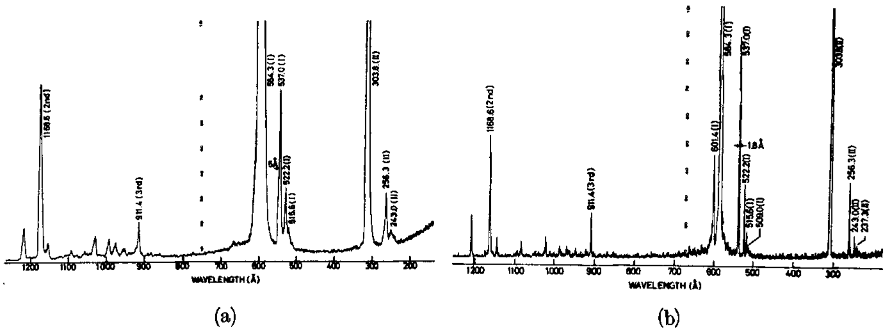

Fig. 13. Photo-electric recordings of emission spectra from the hollow-cathode light source with the HTV-595 electron multiplier (w=40 μm). (a) slit height h=8 mm, effective area A of the HG=30×30 mm; (b) h=1.2 mm, A=10×10 mm.

and V=18 kV. The spectrum shows many highly-ionized Al-lines.

Figure 13 (a and b) gives examples of photo-electric recordings of emission spectrum from the hollow-cathode light source with equal widths, w=40 μm, of the entrance and exit slits for h=8 mm, A=30×30 mm and for h=1.2 mm, A=10×10 mm, respectively. The spectrum is very much improved from (a) to (b). A reciprocal linear-dispersion was experimentally determined on spectrograms as 18 Å/mm, 17 Å/mm and 13 Å/mm for λ=200, 500 and 1000 Å, respectively. The spectrum (b), with the very limited condition for the slit-height and the HG effective area, shows a resolution consistent with the above dispersion, as seen by the line-width 1.5 Å of the HeI 537 Å line.

3-3 Conclusion

The data on the spectrometer SGX-100 in 3-1 have proved that this grazing-incidence spectrometer gives high-quality spectra in photographic as well as photo-electric recordings of plasma emissions. The changeability of the incident angle α (80° to 86°) under a constant line of sight of the spectrometer makes it easy to select the most adequate angle α for the measurements of plasma spectra with a given grating. In general, both gratings and light sources have a varity of characteristics, and so the changeability of the angle α is considered to be very useful for the observation of plasmas in the XUV.

The data on the spectrometer GIT-30 in 3-2 have shown that this small grazing-incidence spectrometer with the toroidal HG is not adequate for the observation of fine spectra with the full ruled-area (30×30 mm) of the HG and the full height (10 mm) of the slits. In spite of the relatively small F-number of the spectrometer as well as of the high through-put of the HG, the spectrometer must be used under a very limited condition to give a linear dispersion of spectra calculated for the slit widths employed. The effective area must be limited, particularly in the vertical direction, for the toroidal HG, and the height must be made small enough for the slits to satisfy the condition. However, the spectrometer is very convenient to use because of its small size and simple mechanism of wavelength scanning. The spectrometer is applicable as a spectrograph to observe the qualitative spectroscopic nature of radiation from light sources. It is also applicable as a monochromator to make photo-electric recordings of absorption or emission spectra of various media in the XUV.

References

1) E. Hinnov: Phys. Rev. **A14** (1976) 1533.
2) TFR Group: Nuclear Fusion **15** (1975) 1053.
3) TFR Group: Report EUR-CEA-FC 861 (1976).
4) M. Klapisch, N. Schweitzer, M. Finkenthal and J.L. Schowb: to be published in J. Opt. Soc. Am.
5) R.U. Datla, M. Blaha and H.-J. Kunze: Phys. Rev. **A12** (1975) 1076.
6) R.U. Datla, L.J. Nugent and H.R. Griem: Phys. Rev. **A14** (1976) 979.
7) I.A. Sellin and D.J. Pegg ed: Beam-Foil Spectroscopy (Plenum Press, New York, 1975) vols. 1 and 2.
8) R.C. Fawcett: Advances in Atomic and Molecular Processes, eds. D.R. Bates and B. Bederson (Academic Press, New York, 1974) vol. 10, p. 223.
9) A.J. Gabriel, J.R. Swain and W.A. Walker: J. Sci. Instrum. **42** (1965) 94.
10) D.O. Landon: Appl. Opt. **3** (1964) 115.
11) M. Neiger and H.R. Griem: Phys. Rev. **A14** (1976) 291.
12) J.R. Van Zadnt, J. Adcock, Jr. and H.R. Griem: Phys. Rev. **A14** (1976) 2126.
13) M.W.D. Mansfield, N.J. Peacock, C.C. Smith, M.G. Hobby and R.D. Cown: J. Phys. **B11** (1978) 1521.
14) R.J. Speer, R.L. Johnson and D. Turner: Vth Int. Conf. on VUV Radiation Phys. Ext. Abst. (Montpelier, France, 1979) Vol. III p. 55.
15) D. Lepere, G. Passereau and A. Thevenon: Vth Int. Conf. on VUV Radiation Phys. Ext. Abst. Vol. III (Montpelier, France, 1979) p. 67.
16) Y. Petroff, P. Thiry, R. Pinchaux and D. Lepere: Vth Int. Conf. on VUV Radiation Phys. Ext. Abst. (Montpelier, France, 1979) Vol. III, p. 70.
17) K. Fukuda, H. Suemitsu and M. Ota: Japan. J. appl. Phys. **13** (1974) 463.
18) K. Fukuda and H. Suemitsu: Vth Int. Conf. on VUV Radiation Phys. Ext. Abst. (Montpelier, France, 1979) Vol. III, p. 138.
19) H. Suemitsu, Y. Matsuura, F. Nako and K. Fukuda: Mem. Fac. Eng. Kyoto Univ. **38** (1976) 255.
20) K. Fukuda and H. Suemitsu: J. Phys. Soc. Japan, **43** (1977) 2109.
21) Y. Hashino, H. Suemitsu and K. Fukuda: Japan. J. appl. Phys. **11** (1972) 710.
22) J.M. Mather: Phys. of Fluids, **8** (1965) 366.
23) N.J. Peacock, R.J. Speer and M.G. Hobbt: J. Phys. **B2** (1969) 798.
24) W.R. Hunter, A.J. Caruso and J.G. Timothy: Vth Int. Conf. on VUV Radiation Phys. (Montpelier, France, 1979) Vol. III, p. 23.
25) K. Fukuda, H. Suemitsu and K. Wani: Japan. J. appl. Phys. **19** (1980) to be published in No. 3.